Investigating the N = 28 shell closure below Z = 20 through ^{47}K(d,p)^{48}K

C. Paxman[1], A. Matta[2], W.N. Catford[1]
& the MUGAST-AGATA-VAMOS collaboration

[1] Department of Physics, University of Surrey, Guildford, GU2 7XH, United Kingdom

[2] Normandie Univ, ENSICAEN, UNICAEN, CNRS/IN2P3, LPC Caen, 14000 Caen, France

GANIL Colloque, 2021

Motivation

Experiment

Analysis

Why N = 28?

First magic number not replicated by just two-body NN [1].

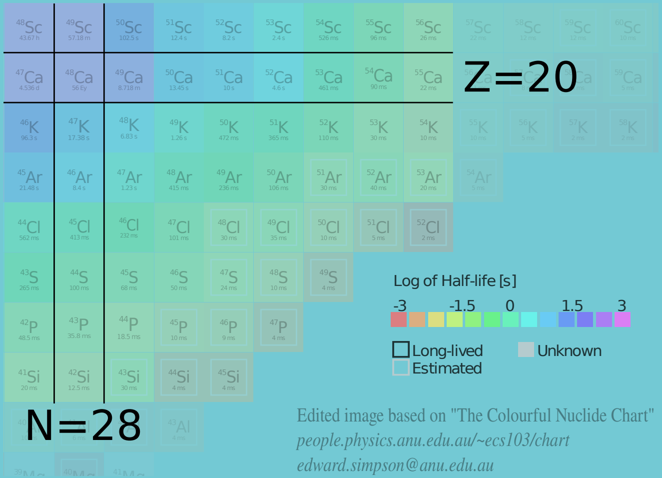

Edited image based on "The Colourful Nuclide Chart"
people.physics.anu.edu.au/~ecs103/chart
edward.simpson@anu.edu.au

[1] J.D. Holt *et al.*, J. Phys. G 39, 085111 (2012)

Why N = 28?

First magic number not replicated by just two-body NN [1].

Weakens Z < 20 [2], gradual deformation.

[2] L.A. Riley *et al.*, Phys. Rev. C 101, 059902 (2020)

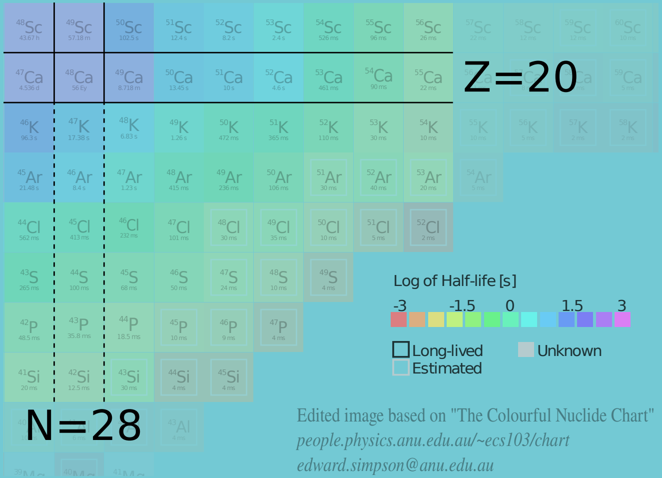

Why N = 28?

First magic number not replicated by just two-body NN [1].

Weakens Z < 20 [2], gradual deformation.

Evidence 54Ca is doubly-magic [3].

[3] D. Steppenbeck *et al.*, Nature 502, 207 (2013)

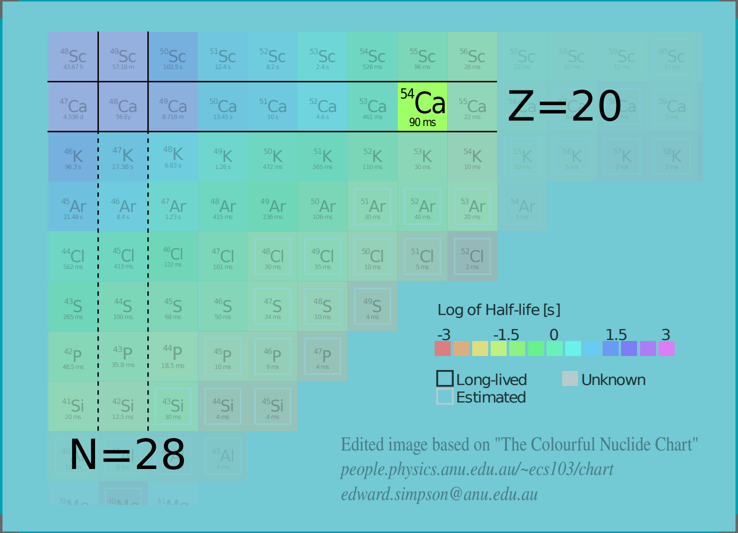

Why N = 28?

First magic number not replicated by just two-body NN [1].

Weakens Z < 20 [2], gradual deformation.

Evidence 54Ca is doubly-magic [3].

[3] D. Steppenbeck *et al.*, Nature 502, 207 (2013)

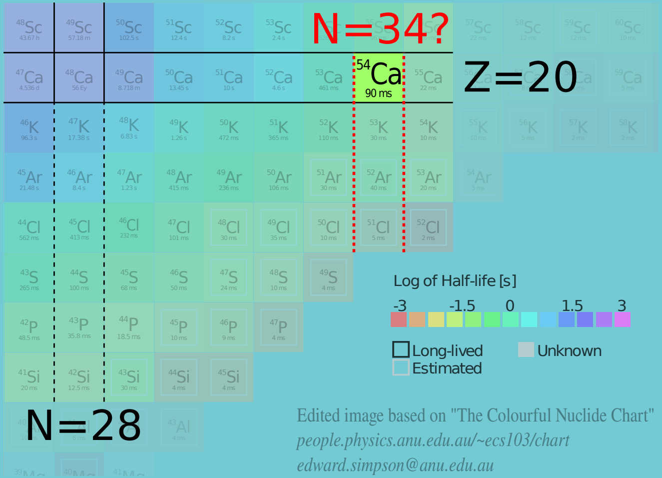

Edited image based on "The Colourful Nuclide Chart"
people.physics.anu.edu.au/~ecs103/chart
edward.simpson@anu.edu.au

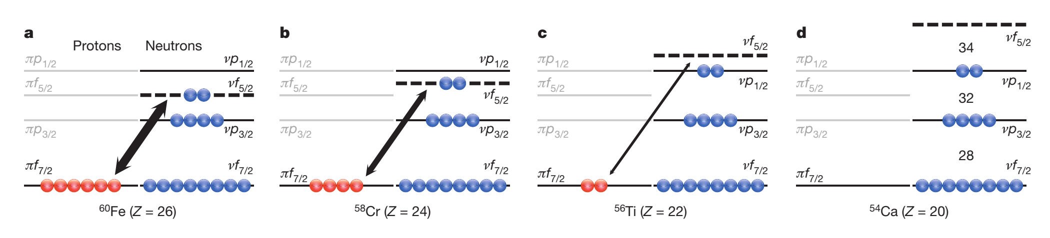

Fig. 1 Emergence of N = 34 magic number. Figure from Ref. [3]. When $\pi f_{\frac{7}{2}}$ is occupied, $\nu f_{\frac{5}{2}} < \nu p_{\frac{1}{2}}$. When $\pi f_{\frac{7}{2}}$ is unoccupied, $\nu f_{\frac{5}{2}} > \nu p_{\frac{1}{2}}$.

Does this persist for isotopes Z<20?

Why ^{47}K(d,p)?

^{48}K is odd-odd & well-positioned.

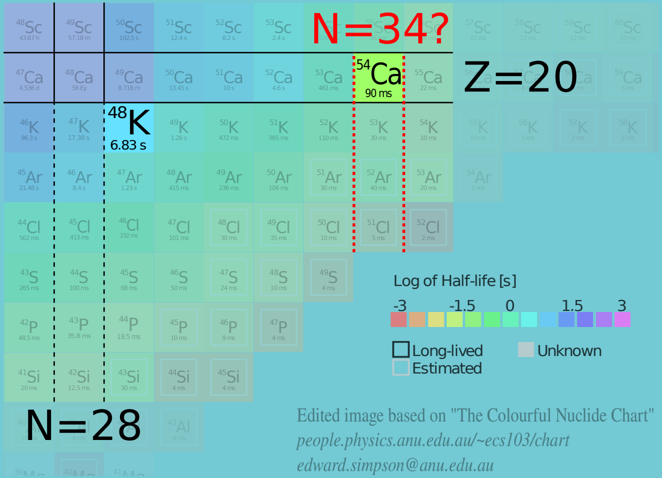

Edited image based on "The Colourful Nuclide Chart"
people.physics.anu.edu.au/~ecs103/chart
edward.simpson@anu.edu.au

Why ^{47}K(d,p)?

^{48}K is odd-odd & well-positioned.

^{47}K structure...

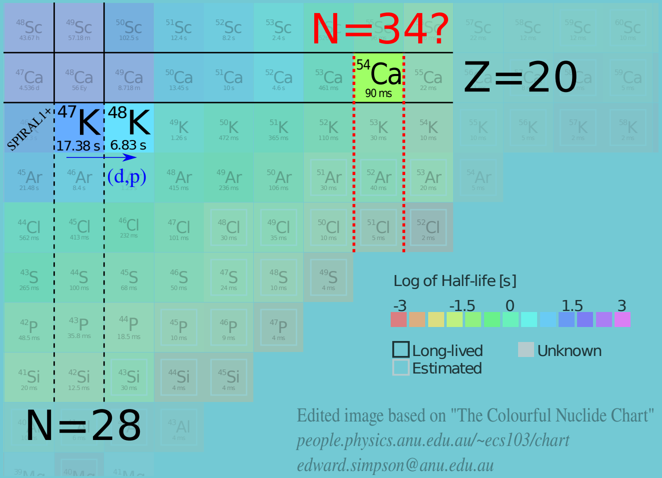

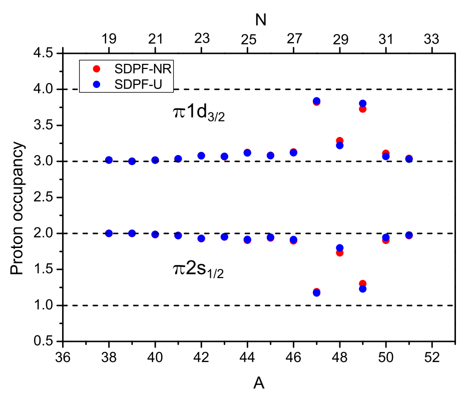

Fig. 2 Proton orbital occupancy in $^{38-51}$K isotopes, figure from Ref. [4]. Note that ^{47,49}K have $\pi(1s_{\frac{1}{2}})^1(0d_{\frac{3}{2}})^4$.

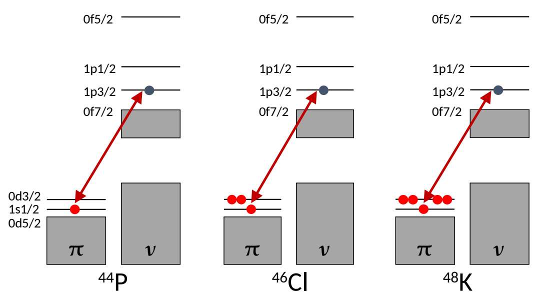

Fig. 3 Low lying states of ^{44}P will be dictated largely by $\pi(1s_{\frac{1}{2}}) \otimes \nu(1p_{\frac{3}{2}})$, which are also populated by ^{47}K(d,p)^{48}K.

[4] J. Papuga et al., Phys. Rev. C 90, 034321 (2014)

Why ^{47}K(d,p)?

^{48}K is odd-odd & well-positioned.

^{47}K structure...
$\ldots\pi(1s_{\frac{1}{2}})^1, \pi(0d_{\frac{3}{2}})^4$

- Predictive of ^{46}Cl and ^{44}P structure.
- Informative about $\nu(fp)$ states.

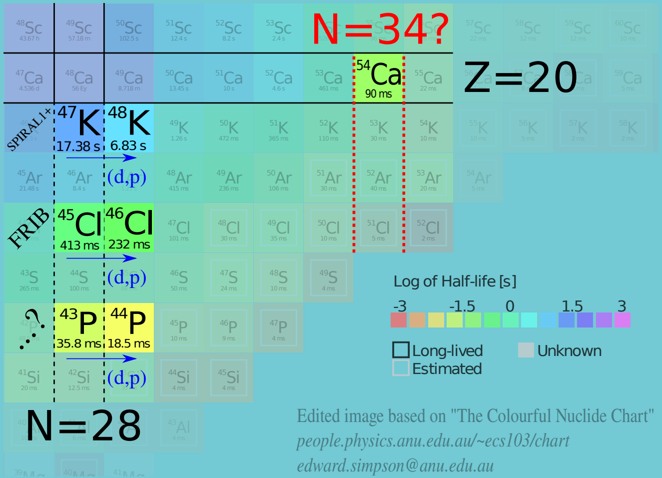

Motivation

Experiment

Analysis

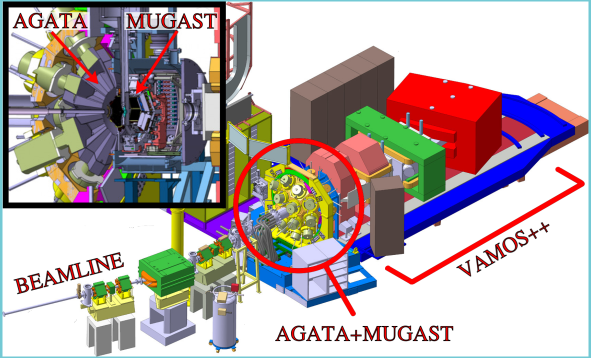

Fig. 4 AGATA-VAMOS coupling (Ref. [5]) with inlay showing AGATA-MUGAST coupling (Ref. [6]).

Overview

- March 2021
- GANIL-SPIRAL1+
- ^{47}K RIB
  - 7.7 MeV/nucl.
  - $\approx$ 99.99% pure
  - $\approx 5 \times 10^5$ pps
- 0.5 mg/cm^2 CD_2 target
- MUGAST + AGATA + VAMOS campaign

[5] E. Clement *et al.*, NIM. A 855, 1-12 (2017).
[6] M. Assié *et al.*, NIM. A 1014, 165743 (2021).

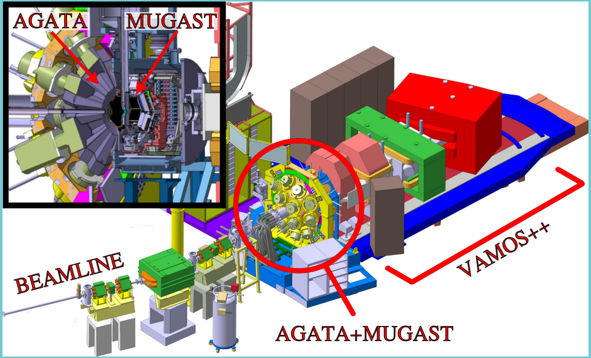

Fig. 4 AGATA-VAMOS coupling (Ref. [5]) with inlay showing AGATA-MUGAST coupling (Ref. [6]).

Overview

- March 2021
- GANIL-SPIRAL1+
- ^{47}K RIB
  - 7.7 MeV/nucl.
  - $\approx$ 99.99% pure
  - $\approx 5 \times 10^5$ pps
- ~~0.5 mg/cm^2~~ CD_2 target
- MUGAST + AGATA + VAMOS campaign

[5] E. Clement *et al.*, NIM. A 855, 1-12 (2017).
[6] M. Assié *et al.*, NIM. A 1014, 165743 (2021).

Detectors

MUGAST

- GRIT + MUST2
- Upstream DSSD's for protons
- Downstream & 90° MUST2 detectors
- High-quality particle spectroscopy
- Viewed through gates on...

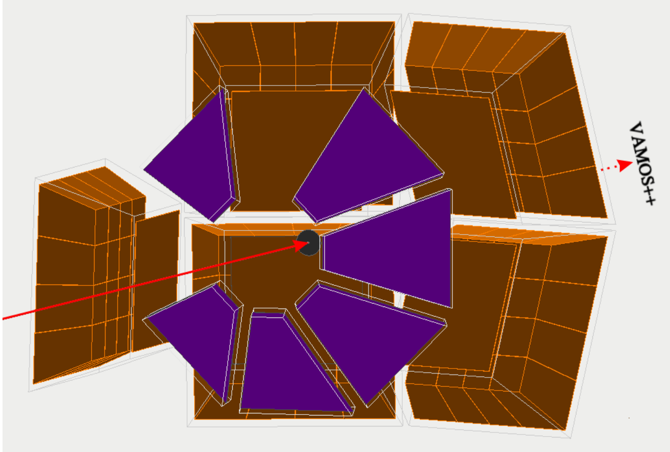

Detectors

MUGAST

- GRIT + MUST2
- Upstream DSSD's for protons
- Downstream & 90° MUST2 detectors
- High-quality particle spectroscopy
- Viewed through gates on...

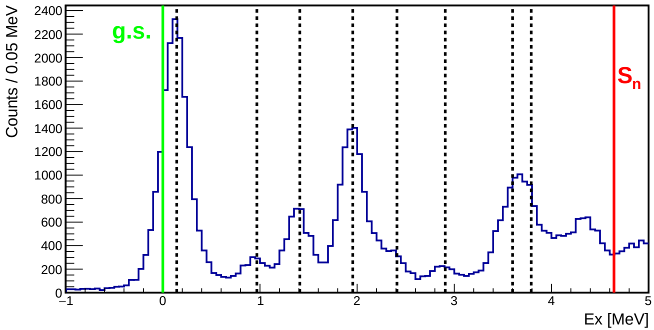

Detectors (cont.)

AGATA

- 12 ATC's → 36 HPGe crystals
- Precise γ-ray gating and γ-γ coincidence
- FWHM $\approx$ 0.01 MeV @ 1.8 MeV

VAMOS++

- Timing gate
- Reject reactions on C

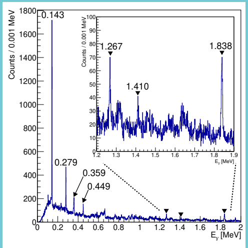

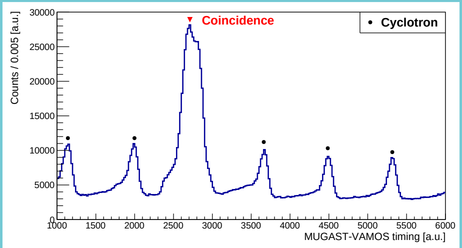

Motivation

Experiment

Analysis

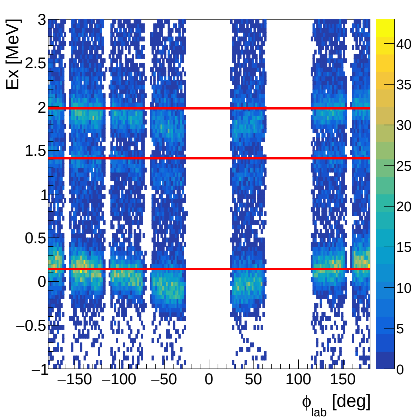

Fig. 6 Sinusoidal variation in energy across MUGAST trapezoids due to beam offset.

Corrections

Beam off-centre → MUST2 shift to negative X, MUGAST misaligned...

Thin target → expected vs detected particles.

Aligning 0.143 *MeV* peak in MUGAST detectors:

- X = −3.92 *mm*
- Y = +0.06 *mm*
- Z = +1.06 *mm*
- T = 0.187 mg/cm^2

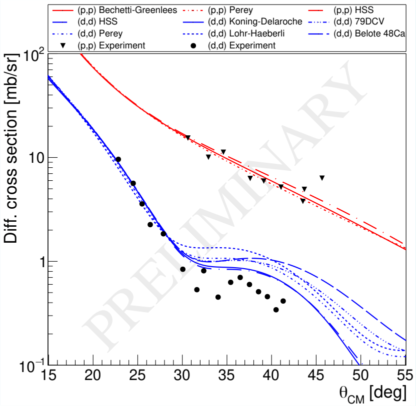

Fig. 7 Experimental elastic scattering data, compared to various optical models.

Corrections

Beam off-centre → MUST2 shift to negative X, MUGAST misaligned...

Thin target → expected vs detected particles.

Using elastics to determine target thickness:

- $CD_2 = 0.18(1)\ mg/cm^2$
- $CH_2 = 0.01(1)\ mg/cm^2$
- ∴ $T = 0.19(2)\ mg/cm^2$

Methods agree, 37% of nominal.

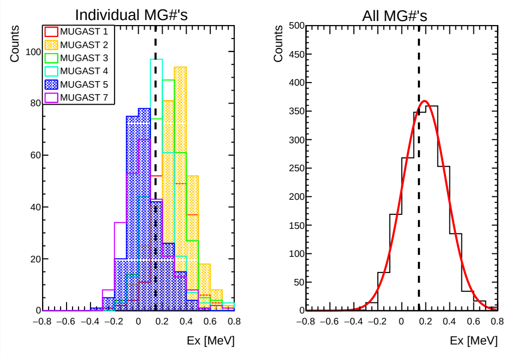

(a) Before correction, FWHM= 0.423(7) *MeV*

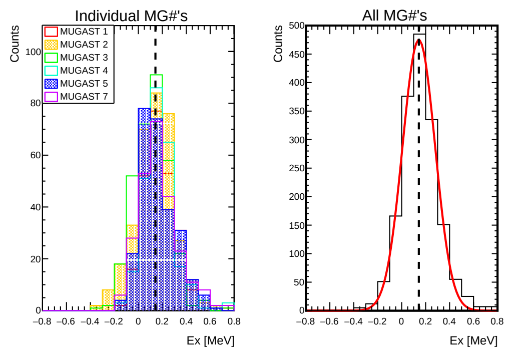

(b) After correction, FWHM= 0.321(7) *MeV*

Fig. 8 Comparison of the 0.143 *MeV* excited state, isolated through γ-gating, as seen by the individual MUGAST detectors (left, $a\&b$) and the sum of the detectors (right, $a\&b$).

Level scheme

Analysis performed using **nptool**.

Triple-coincidence is vital.

Currently...

- Six new states
- Nine new transitions
- Two tentative spin-parities

Believed to arise from $\pi(1s_{\frac{1}{2}}) \bigotimes \nu(fp)$.

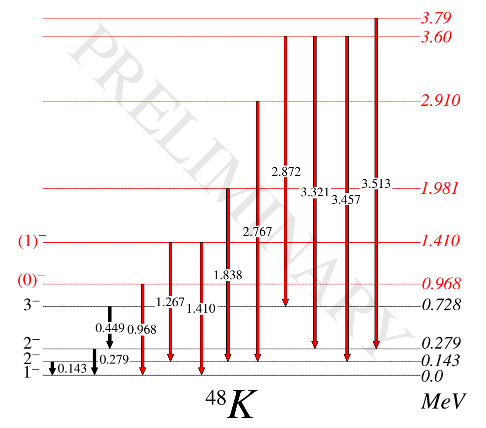

Fig. 9 Preliminary level scheme derived from this work. New states/decays shown in red.

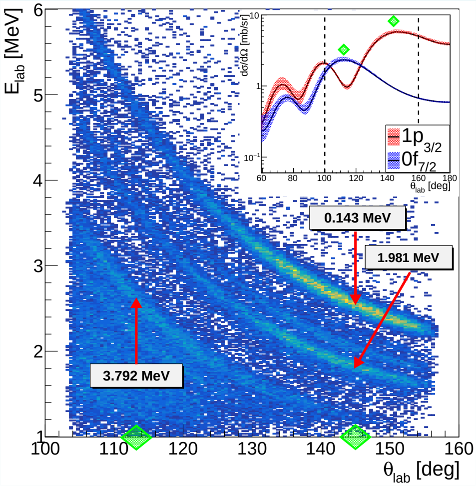

Fig. 10 Proton energy against lab angle, where the kinematic lines correspond to states in the final nucleus. Inlay shows predicted diff. cross sections (TWOFNR).

To do:

- More states (especially 4-4.6 *MeV*).
- Differential cross sections.
- Spectroscopic factors.
- Branching ratios.

Thank you!

C. Paxman[1], W.N. Catford[1], A. Matta[2], D.T. Doherty[1], M. Assié[3], E. Clément[4], A. Lemasson[4], D. Ramos[4], F. Galtarossa[3], L. Achouri[2], D. Ackermann[4], D. Beaumel[3], L. Canete[1], P. Delahaye[4], J. Dudouet[5], B. Fernández-Domínguez[6], D. Fernández-Fernández[6], F. Flavigny[2], C. Fougères[4], G. de France[4], S. Franchoo[3], J. Gibelin[2], N. Goyal[4], F. Hammache[3], D.S. Harrouz[3], B. Jacquot[4], L. Lalanne[3 4], C. Lenain[2], J. Lois-Fuentes[6], T. Lokotko[2], F.M. Marqués[2], I. Martel[7], N.A. Orr[2], L. Plagnol[2], D. Regueira-Castro[6], N. de Séréville[3], J.-C. Thomas[4], A. Utepov[4].

[1] *Univ. Surrey*
[2] *LPC Caen*
[3] *IJCLab*
[4] *GANIL*
[5] *IP2I Lyon*
[6] *Univ. Santiago de Compostela*
[7] *Univ. Huelva*

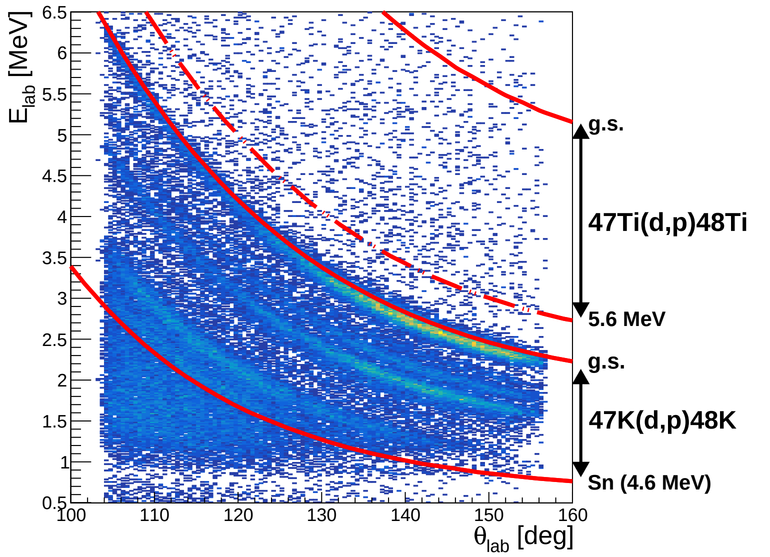

E_{lab} [MeV]
6.5
6
5.5
5
4.5
4
3.5
3
2.5
2
1.5
1
0.5
100
110
120
130
140
150
160
θ_{lab} [deg]
g.s.
47Ti(d,p)48Ti
5.6 MeV
g.s.
47K(d,p)48K
Sn (4.6 MeV)

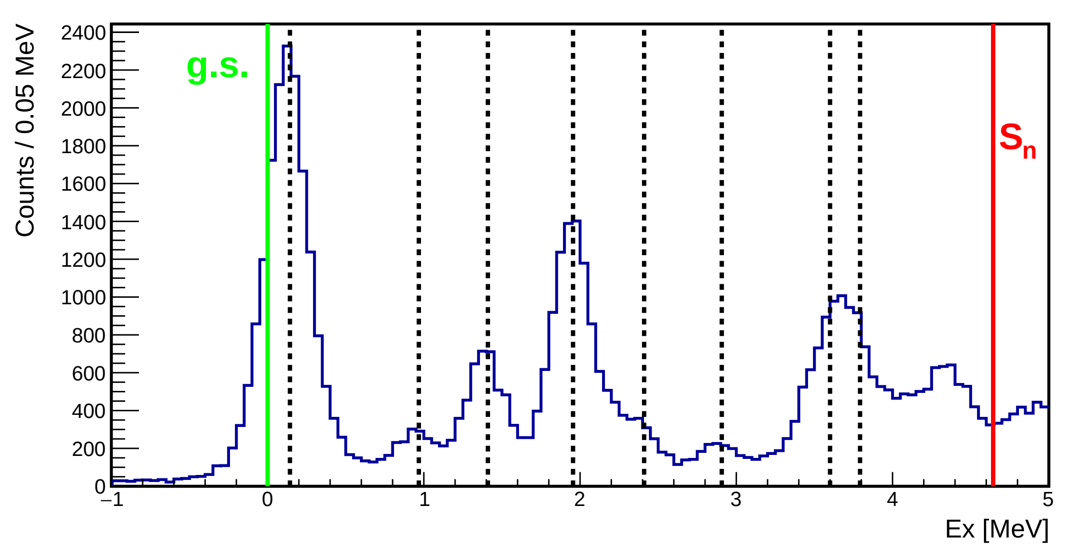

Counts / 0.05 MeV
2400
2200
2000
1800
1600
1400
1200
1000
800
600
400
200
0
−1
0
1
2
3
4
5
Ex [MeV]
g.s.
S_n

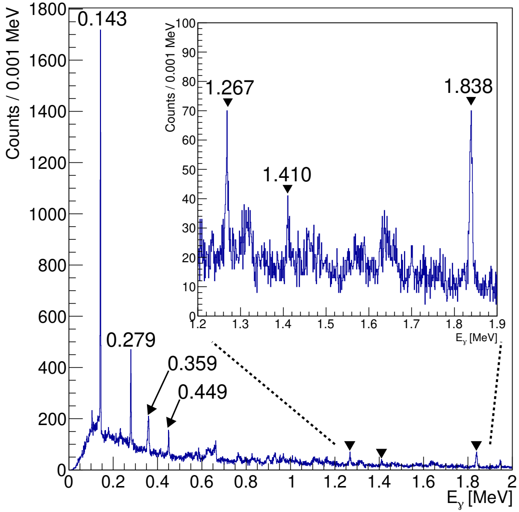

Counts / 0.001 MeV
E$_\gamma$ [MeV]
0.143
0.279
0.359
0.449
1.267
1.410
1.838